

Gas Transport Properties in Cross-Linked and Vacuum Annealed Poly(oxyindole biphenylene) Membranes

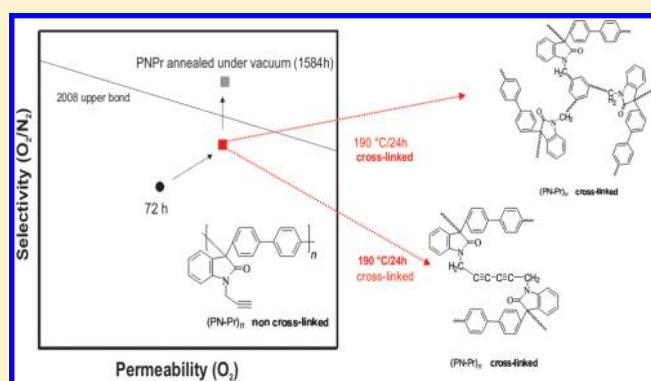
Jesús Ortiz-Espinoza,[†] F. Alberto Ruiz-Treviño,^{*,†,‡} Hugo Hernández-Martínez,[†] Manuel J. Aguilar-Vega,^{‡,§} and Mikhail G. Zolotukhin^{§,¶}

[†]Departamento de Ingeniería y Ciencias Químicas, Universidad Iberoamericana, Prol. Paseo de la Reforma No. 880, Lomas de Santa Fe, 01219 Ciudad de México, Mexico

[‡]Unidad de Materiales, Centro de Investigación Científica de Yucatán, A. C., Calle 43 por 32 y 34 No. 130, Chuburná de Hidalgo, 97205 Mérida, Yucatán, Mexico

[§]Instituto de Investigación en Materiales, Universidad Nacional Autónoma de México, Apartado Postal 70-360, CU, Coyoacán, 04510 Ciudad de México, Mexico

ABSTRACT: This work studies useful routes to produce cross-linked poly(oxyindole biphenylene) bearing a cross-linkable propargyl group, PNPr. Thus, the effect of cross-linking temperature and time on gas permeability and ideal selectivity for a non-cross-linked PNPr membrane to produce a cross-linked PNPr membrane is studied in detail in order to learn how more productive membranes, in terms of permeability–selectivity combinations, and membranes resistant to solvent swelling and CO₂ plasticization may be produced. Systematic studies on structure/processing/property relationship assessed by Fourier transform infrared attenuated total reflectance (FTIR-ATR), gel content (GC [%]), swelling degree (SD [%]), specific volume, wide-angle X-ray diffraction (WAXD), and gas permeability measurements reveal that PNPr membranes cross-linked under vacuum (1 mmHg) at 190 °C for 24 h, and further vacuum-annealed for 1584 h, at 35 °C and 10^{−3} mmHg, produce membranes that overcome the typical trade-off between permeability and selectivity. In effect, the thermally cross-linked membranes annealed under vacuum for 1584 h, as compared to the non-cross-linked membranes, possess $P(\text{H}_2)$ and $P(\text{CO}_2)$ that increase by 2.4 and 2.1 factors while selectivity increases from 25 to 45 for the H₂/CH₄ pair and from 25 to 39 for the CO₂/CH₄ pair, whereas $P(\text{O}_2)$ increases by a 2.4 factor with an associated increase in selectivity from 4.4 to 9.6 for O₂/N₂ which situates this membrane above Robeson's 2008 upper-bound limit, at least for this pair of gases. The cross-linked membranes are resistant to solvent swelling, since their SD [%] in NMP is on the order of 1–3%, and also to CO₂ plasticization since the plasticization pressure was not observed at least up to the 18 bar upstream pressure studied here.



1. INTRODUCTION

Gas polymer membrane separation technology is an attractive alternative since it is based on the relative magnitude of the gas permeability coefficients to be separated, and mainly because it can be carried out at relatively low temperature and pressure as compared to other current separations.^{1–4} However, if amorphous polymer membranes want to find generalized application in real situations, they need to be productive in terms of their permeability–selectivity combination,^{5–7} in addition to possessing resistance to solvent swelling and CO₂ plasticization. In effect, the current literature presents a great variety of interesting polymers with an attractive permeability–selectivity combination, such as 6FDA-DAM:DABA,⁸ Matrimid,⁹ HAB-6FDA,¹⁰ KAUST-PI-1,¹¹ and PIMs;¹² however, their gas transport and separation properties could change due to solvent swelling, aging, or densification, and/or owing to plasticization promoted by high condensable gases such as

CO₂.^{13–17} It is well-known that all of these changes are associated with changes in free volume due to the amorphous nature of polymer membranes.¹⁸ Thus, an interesting challenge for science and engineering is to learn how changes in free volume, defined as a difference between the amorphous specific volume at given temperature, $V_g(T)$, minus the corresponding specific volume at equilibrium, $V_c(T)$, may be ideally suppressed or at least mitigated.

Thermal treatments and/or cross-linking to change the chemical structure or the solid-state packing of glassy polymers are attractive routes to produce polymer membranes that fulfill all or at least some of the mentioned requirements. Chung¹⁹ et

Received: June 19, 2018

Revised: August 10, 2018

Accepted: August 23, 2018

Published: September 5, 2018

al. studied the effect of thermal treatments, between 150 and 320 °C, on the CO₂ plasticization pressure of 6FDA-2,6-DAT hollow fibers, and determined that plasticization can be suppressed up to 14.6 bar upstream pressure, as a consequence of a better chain packing and nodule interaction promoted by annealing at high temperatures. In the direction of cross-linking, Koros and co-workers reported cross-linked polyimide membranes with high resistance to plasticization pressures.^{20–22} An alternative approach is also to promote chemical changes, by high temperature treatments, in the polymer structure to increase the rigidity of the polymer chains, while maintaining large interchain spacing, as it has been learned from the so-called thermally rearranged polymers and polymers with intrinsic microporosity (PIMs) that results in a more rigid backbone.^{23,24} Moreover, in a previous work Hernández-Martínez²⁵ et al. showed that a simultaneous thermal cross-linking and decomposition of side groups located strategically in a poly(oxyindole biphenylene) copolymer may lead to gas separation membranes that are more resistant to physical aging, thus more resistant to changes in their gas transport properties. Particularly in this work, a poly(oxyindole biphenylene) bearing just a cross-linkable propargyl group (PNPr) membrane is synthesized in order to study the net effect of cross-linking processing variables, such as temperature and time, on the permeability–selectivity combination of the resulting cross-linked membranes. The systematic structure/processing/property relationship is assessed by Fourier transform infrared attenuated total reflectance (FTIR-ATR), gel content (GC), swelling degree (SD), specific volume, wide-angle X-ray diffraction (WAXD), and gas permeability coefficients to learn how to produce a more productive and more resistant cross-linked PNPr membrane.

2. EXPERIMENTAL SECTION

2.1. Materials and Polymer Synthesis. 2.1.1. Materials.

All starting materials were purchased from Aldrich Chemical. Propargyl bromide (BrPr) and potassium carbonate (K₂CO₃) were used as received, whereas *N*-methyl-2-pyrrolidinone (NMP) was distilled before use.

2.1.2. Polymer Synthesis. Figure 1 summarizes the chemical reaction pathway to synthesize a poly(oxyindole biphenylene-

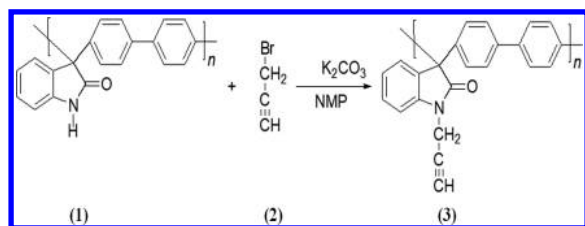


Figure 1. Chemical reaction pathway to synthesize, at room temperature, pure poly(oxyindole biphenylene) bearing a cross-linkable propargyl group, PNPr (3).

lene) bearing a cross-linkable propargyl group, PNPr (3), which will be used as a model to study the effect of temperature and time on the permeability and selectivity properties of the resulting membranes. The chemical reaction that can be carried out at room temperature involves an already synthesized poly(oxyindole biphenylene) that bears a hydrogen atom, PNH (1) polymer, reacted with propargyl bromide (2). A typical synthesis is as follows: In a single-necked flask equipped with a magnetic stirrer, fibrous PNH

(0.25 g, 0.88 mmol) is dissolved with NMP (2.5 mL). Once dissolution is reached, known amounts of K₂CO₃ (0.6095 g, 4.4 mmol) and BrPr (0.4836 mL, 4.4 mmol) are added, and the mixture is reacted, at room temperature, for 24 h or until a red color, high viscosity solution is formed. Afterward, the polymer is precipitated in methanol, as white fibers, and washed several times in acid water (pH 6) until the residual water becomes pH 7. The polymer is then Soxhlet extracted with methanol/water solutions to remove the residual NMP. For the typical reaction described the yield of PNPr was 0.257 g.

2.2. Membrane Formation and Thermal Treatments.

Polymer dense films were solution-cast onto a horizontal surface of cellophane using chloroform solutions containing 3 wt % polymer. The cast films were dried overnight and then removed from the cellophane to be further vacuum-dried for an additional 24 h at 80 °C to remove residual solvent. The thicknesses of pure polymer films, the so-called non-cross-linked polymer, were between 20 and 30 μm. To produce the cross-linked polymer as-cast membranes were treated under vacuum (~1 mmHg) at different temperatures (150, 170, 190, and 210 °C) and maintained at the oven temperature for different times (1 and 24 h), using an standardized thermal protocol that was defined as follows: (1) the vacuum oven, a Yamato ADP 21, was equilibrated (~20 min) at the desired temperature; (2) the membrane was then introduced for the desired time; (3) the membrane was removed from the vacuum oven and allowed to cool until it reached room temperature.

2.3. Polymer Membrane Characterization.

Proton nuclear magnetic resonance (¹H NMR) was used to verify the chemical structure of the synthesized poly(oxyindole biphenylene) that bears a propargyl group (PNPr) in a Bruker Avance spectrometer. The chemical cross-linking reaction throughout the thermolabile propargyl groups was followed indirectly by measuring the gel content, GC [%] = (M_c/M₀) × 100, and the swelling degree in NMP, SD [%] = (M_s/M_c) × 100,²⁶ where M_c is the weight of an already cross-linked polymer, M₀ is the weight of initially dried membrane, made up a fraction of non-cross-linked and cross-linked polymer, and M_s is the weight of NMP adsorbed at equilibrium in the cross-linked polymer. Similarly, FTIR-ATR, in a Nicolet iS10, was also used to get the corresponding spectra in the non-cross-linked and cross-linked membranes. All spectra were normalized using the software OMNIC 8.0. For all membranes, the specific volumes of dried films, V(30 °C), were measured at 30 °C in a density gradient column using well-degassed ZnCl₂ solutions. Wide-angle X-ray diffraction (WAXD) scans were made for non-cross-linked and cross-linked membranes using a Xeuss Xenocs X-ray diffractometer at a Cu K wavelength of 1.54 Å. A corresponding *d*-spacing, as an indicator of the average chain spacing which it is known indirectly correlates with fractional free volume, was calculated from the diffraction peak maxima using the well-known Bragg's equation, $n\lambda = 2d \sin \theta$. Permeability coefficients, *P*(*i*), for ultra-high-purity gases H₂, O₂, N₂, CH₄, and CO₂, were measured, at 35 °C and 2 bar, in all membranes after 72 h of any thermal treatment. All *P*(*i*) were measured in a variable pressure/constant volume permeation cell following a well-established procedure reported elsewhere.²⁷ For this work, ideal selectivity for two gas pairs, *i* and *j*, is defined as the ratio of two pure gas permeability coefficients, *P*(*i*)/*P*(*j*). Specifically, the effect of aging time on the *P*(*i*) of an already cross-

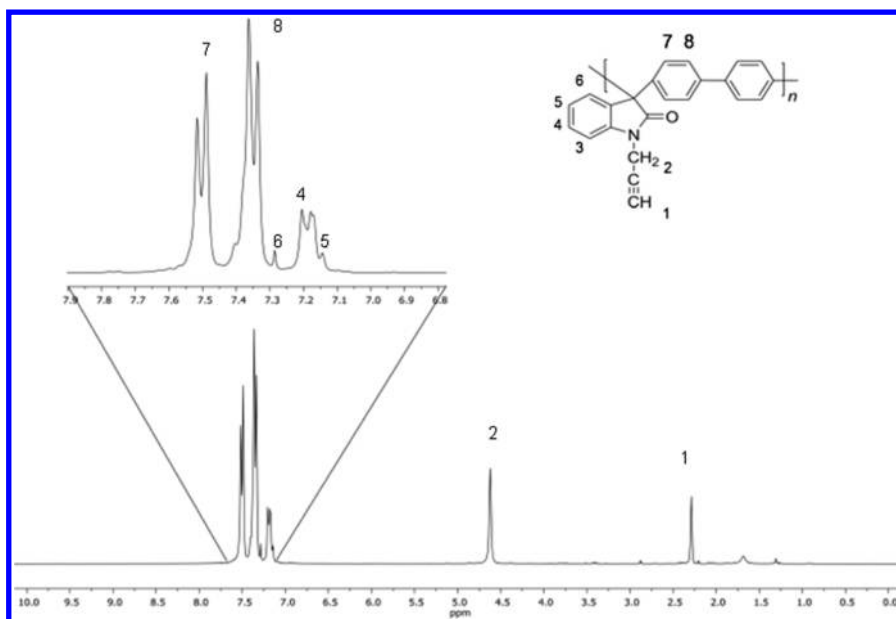


Figure 2. ^1H NMR spectrum for synthesized PNPr polymer (solution in CDCl_3).

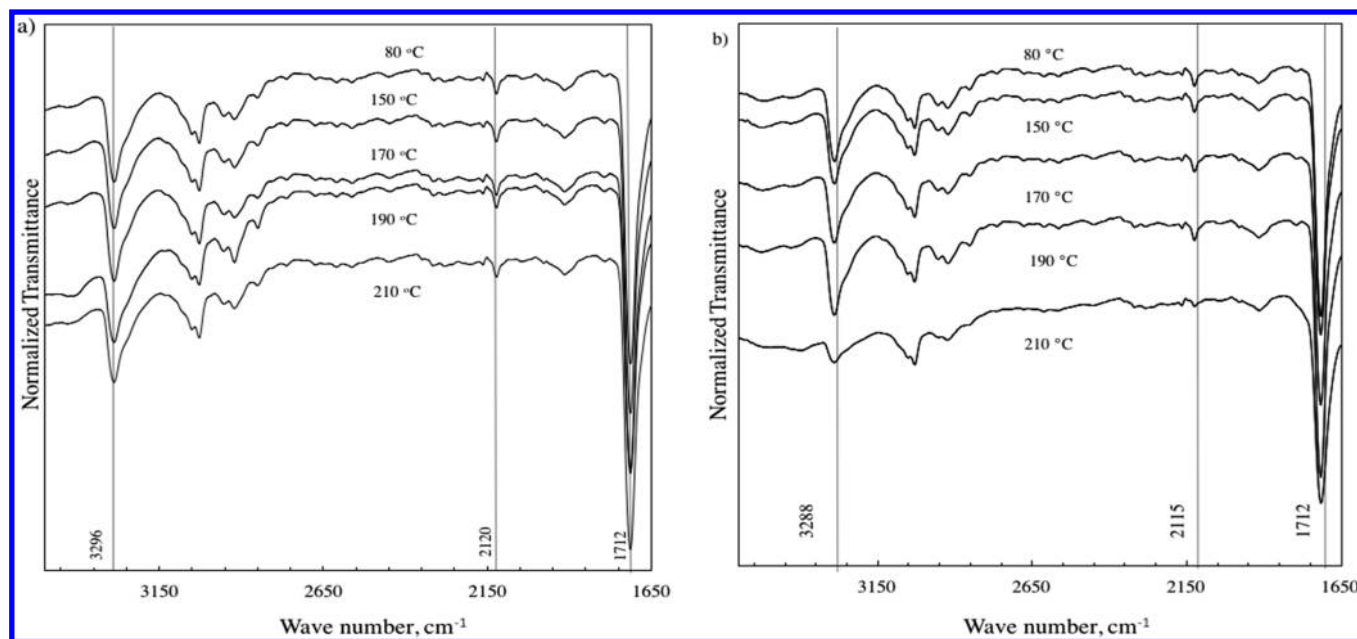


Figure 3. FTIR-ATR spectra for pure PNPr and for PNPr membranes thermally treated at different temperatures for 1 (a) and 24 h (b).

linked membrane was followed for at least 1584 h, maintaining always the membrane at $35\text{ }^\circ\text{C}$ under a relatively high vacuum (10^{-3} mmHg).

3. RESULTS AND DISCUSSION

3.1. Polymer Synthesis. Figure 2 shows a characteristic ^1H NMR spectrum determined for a poly(oxyindole biphenylene) bearing a cross-linkable propargyle group synthesized following the reaction scheme described in Figure 1. Signals at 2.25 and 4.65 ppm correspond to propargyl protons, whereas the doublets at 7.35 and 7.51 ppm are representative of biphenyl protons. The remaining signals correspond to the rest of the protons that make up the polymeric repeating unit. The ^1H NMR analysis confirms the chemical reaction scheme depicted in Figure 1, where the

hydrogen atom of polymer PNH^{28} has been completely replaced by the propargyl group to produce a PNPr, a poly(oxyindole biphenylene) that contains propargyl as a lateral group.

3.2. Membrane Formation and Thermal Treatments.

The progress of the cross-linking reaction in PNPr, at different temperatures and times, was followed by FTIR-ATR analysis as described in Figure 3, part a for 1 h and part b for 24 h thermal treatments. Important signals are located at 3296 cm^{-1} , associated with acetylene vibrations, and 2120 cm^{-1} , which corresponds to the $\text{C}\equiv\text{C}$ vibrations.^{29–32} The area for each signal diminishes as the temperature increases, corroborating the cross-linking reaction between, or among, the propargyl groups. The cross-linking reaction of propargyl groups has been widely studied in air and inert atmospheres at temperatures higher than $200\text{ }^\circ\text{C}$, showing that it can proceed

under simultaneous complex mechanisms. In this work, the cross-linking reaction, carried out under vacuum (~ 1 mmHg) at lower temperatures than those reported in air, would be expected to proceed at least with two possible mechanisms: one that implies a simple trimerization reaction among three acetylene end groups to form an aromatic cross-linker as depicted in mechanism a reported in Figure 4, and another one

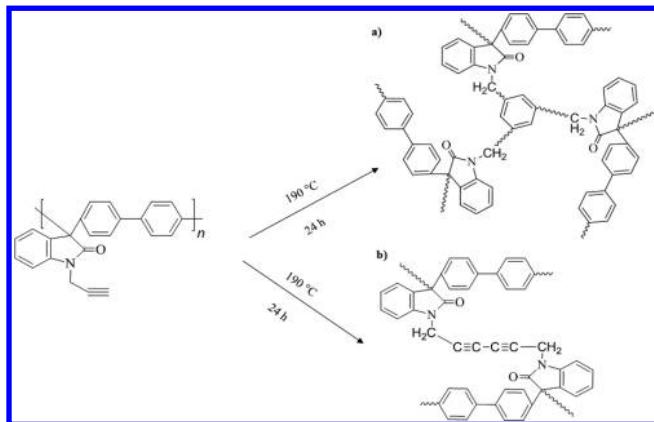


Figure 4. Simultaneous chemical reaction mechanism to produce cross-linked membrane starting from PNPr polymer membrane that has been thermally treated, under vacuum, at 190 °C for 24 h. Part a implies an aromatic cross-linker, whereas part b implies a linear cross-linker.

that implies a complex coupling reaction through the triple bond in the C–C atoms (Strauss coupling, Glaser coupling) to produce a linear cross-linker as depicted in mechanism b in Figure 4, just as it has been described elsewhere.³² Table 1 summarizes the weight percent of cross-linked polymer, determined as GC [%], the swelling degree (SD [%]), and a “cross-linking degree” (X_{IR} [%]) determined by FTIR-ATR analysis following the reduction in the area associated with the acetylene vibration (at 3296 cm^{-1}) of a cross-linked PNPr membrane with respect to the area determined for a non-cross-

Table 1. Gel Content (GC [%]), Swelling Degree (SD [%]), and Cross-Linking Degree Determined from FTIR-ATR for PNPr and for PNPr Thermally Treated Membranes at Different Temperatures for 1 and 24 h

	cross-linking temp (°C)	GC [%], ^a (NMP)	SD [%] ^b	X_{IR} [%] ^c
PNPr		0	100	0
PNPr, 1 h	150	14.6	85	22
	170	83.3	17	42
	190	96.4	4	56
	210	97.3	3	90
PNPr, 24 h	150	45.4	55	38
	170	89.5	10	55
	190	98.5	2	80
	210	99.0	1	99

^aGC [%] = $(M_c/M_0) \times 100$, where M_0 is the initial weight of dried membrane and M_c is the corresponding weight of a cross-linked membrane. ^bSD [%] = $(M_s/M_c) \times 100$, where M_s is the weight of adsorbed solvent (NMP) in a weight of a cross-linked membrane, M_c . ^c X_{IR} [%] = $(A_i/A_0) \times 100$, where A_i and A_0 are the areas under the FTIR-ATR 3296 cm^{-1} signal associated with the acetylene C–H group of PNPr cross-linked membrane at a given temperature and time, A_i , and a PNPr non cross-linked membrane, A_0 .

linked one. In Table 1, the GC [%] and X_{IR} increase as the cross-linking temperature and time increase; i.e., at 190 °C, the GC [%] of 96.4% for 1 h increases to 98.5% for 24 h, while at 210 °C, the GC [%] increases from 97.3 to 99%. These results confirm that a high content of a cross-linked polymer, under the vacuum conditions studied here, may be obtained in a 190 and 210 °C temperature range to produce highly resistant cross-linked membranes to solvent plasticization since their SD [%], in an aggressive NMP solvent, is in the range 1–3%, as can be seen in Table 1.

Figure 5 shows the WAXD scans for non-cross-linked and cross-linked PNPr membranes at different temperatures for 1 h (part a) and for 24 h (part b). The results reveal two broad peaks that move to the right or left depending on the temperature and time used to carry out the cross-linking reaction. In general, these membranes are constituted by two types of solid state packing: a fraction of efficient chain-to-chain packing attributed to d -spacing between 3.98 and 4.12 Å, a typical range found in glassy polymers, and another fraction loosely packed characterized by d -spacing between 7.75 and 8.02 Å, a typical range reported for PIMs. The exact nature of these two well-defined peaks is not known; however, two well-defined peaks have been reported previously for glassy polymers with pendant phenyl rings such as polystyrene, poly(2,6-diphenyl-1,4-phenylene oxide), glassy polymers with rigid structures such as FBP/tBIA and FBP/IA,³³ and recently for polymers with intrinsic microporosity. In this work, it is assumed that the average d -spacing that corresponds to the efficient chain-to-chain packing could correspond to the fraction of cross-linked polymer where a linear cross-link has been formed, whereas the more loosely packed fraction could correspond to the fraction of cross-linked polymer where an aromatic cross-linker has been formed (see Figure 4). Of course, the fraction distribution is highly dependent on the cross-linking temperature and time conditions.

3.3. Gas Transport Properties. Table 2 summarizes the permeability coefficients and ideal separation factors for several gases, at 35 °C and 2 bar, as well as the specific volume, $V(30\text{ °C})$, and two d -spacing values for non-cross-linked and cross-linked PNPr membranes at different temperatures and times. For all gases, the net effect of increasing the thermal treatment temperature results in an increase of gas permeability coefficients, with an ideal selectivity that remains practically constant or increases depending on the type of gases being permeated; i.e., the membrane that was cross-linked for 24 h at 190 °C increases permeability coefficients for H_2 and O_2 by 2.24 and 2.50 factors, respectively, whereas H_2/CH_4 increases from 25 to 27 and O_2/N_2 increases from 4.4 to 5.2. It is interesting to note that the permeability coefficients for the cross-linked membranes are higher than the corresponding values for the non-cross-linked membranes, even though the cross-linked membranes possess a lower specific volume (see values in Table 2), as is expected for cross-linked membranes. In order to elucidate the net effect of cross-linking on the increases in permeability coefficients, Table 2 summarizes two d -spacing determinations that correspond to the maximum peaks observed in Figure 5. It is assumed in this work that the first d -spacing corresponds to a more loosely packed fraction—the one that contains the bulky connector aromatic group (see mechanism a in Figure 4)—whereas the second one corresponds to a fraction of polymer with a more efficient chain-to-chain packing—the one that contains the linear connector group (see mechanism b in Figure 4). It is also

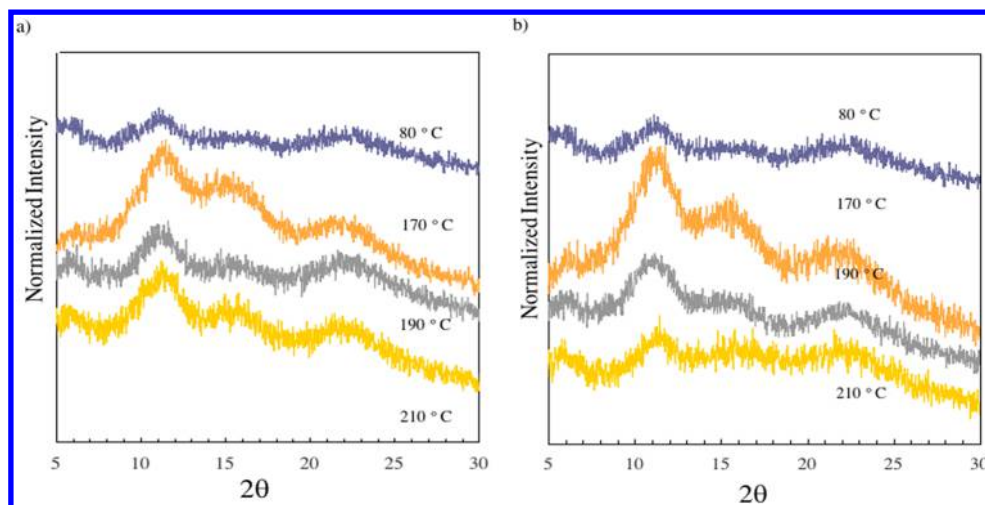


Figure 5. WAXD diffractograms for pure PNPr and for PNPr membranes thermally modified at different temperatures for 1 (a) and 24 h (b).

Table 2. Permeability Coefficients for Pure Gases and Ideal Selectivity, at 35 °C and 2 bar, Specific Volume, $V(30\text{ °C})$, and Two d -Spacing Values Determined for PNPr and for PNPr Membranes Thermally Treated at Different Temperatures for 1 and 24 h

time (h)	cross-linking temp (°C)	permeability, $P(i)^a$					ideal selectivity, $P(i)/P(j)$				$V(30\text{ °C})^b$ (cm ³ /g)	d -spacing ^c (Å)
		H ₂	O ₂	N ₂	CH ₄	CO ₂	H ₂ /CH ₄	CO ₂ /CH ₄	O ₂ /N ₂	CO ₂ /N ₂		
		33	4.0	0.9	1.3	32	25	25	4.4	36	0.883	7.94; 4.00
1	170	44	6.0	1.2	1.7	39	26	23	5.0	33	0.885	7.82; 4.12
1	190	47	6.0	1.2	1.6	46	29	29	5.0	38	0.859	7.90; 4.02
1	210	54	8.0	1.7	2.4	53	23	22	4.7	31	0.881	7.79; 4.12
24	170	43	6.0	1.3	1.6	39	27	24	4.6	30	0.861	7.93; 4.11
24	190	74	10	1.9	2.7	67	27	25	5.2	35	0.835	8.02; 3.98
24	210	54	8.0	1.8	2.5	54	21	21	4.4	30	0.852	7.75; 4.08

^aPermeability in barrer (1 barrer = 1×10^{-10} cm³ gas STP cm/cm²s cmHg). ^bSpecific volume measured at 30 °C in a density gradient column. ^c d -spacing values determined from WAXD using Bragg equation applied to the corresponding two maximum peaks that appear in Figure 5.

important to note that the cross-linking effect is highly dependent on the size and type of gas being permeated. A careful examination in Table 2 between permeability coefficients and the two d -spacing values reveals that the increases in permeability are associated with the increases in the d -spacing distribution of the more loosely packed polymer chains that increases from 7.93 to 8.02 Å, which is perceptible to H₂, O₂, CO₂, and CH₄, whereas the smaller increase in $P(N_2)$ should be associated with a combination of both an increase in the d -spacing distribution of the more loosely packed polymer chains and a reduction in the d -spacing distribution of the more efficient packing fraction of polymer chains that decreases from 4.11 to 3.98 Å. An additional important observation to be noted in Table 2 is that $P(H_2)$ and $P(CO_2)$ are practically the same independently if PNPr membrane is non-cross-linked or cross-linked. It is well-known that $P(H_2) > P(CO_2)$ for amorphous polymers, while it is common to find that $P(H_2) < P(CO_2)$ for polymers with intrinsic microporosity.^{34,35} A more fundamental study is being carried out to learn more about this interesting phenomenon, but a possible explanation could be related to a lower solubility of H₂ in these types of polymers, as compared to typical amorphous polymers.

Figure 6 shows the selectivity–permeability performance for the gas pairs (a) H₂/CH₄, (b) O₂/N₂, (c) CO₂/CH₄, and (d) CO₂/N₂, determined for non-cross-linked PNPr membranes (open squares) and for cross-linked PNPr membranes under

vacuum at 190 °C for 1 and 24 h (black squares). Figure 6 reports the effect of aging time (gray squares) at 35 °C and under a relatively high vacuum (10^{-3} mmHg), on the selectivity–permeability performance of the PNPr cross-linked membrane at 190 °C for 24 h. The 2008 upper-bound limit proposed by Robeson⁶ has also been incorporated as a reference line. The net effect of increasing the cross-linking time results in an increase in permeability without changes in the ideal selectivity for the pairs of gases shown in Figure 6. For example, for the pair of gases H₂/CH₄, $P(H_2)$ increases by 1.42 and 2.24 factors for thermal treatments of 1 and 24 h, and the selectivity holds practically constant at 25–29. For O₂/N₂, $P(O_2)$ increases by 1.5 and 2.5 factors for 1 and 24 h, and the selectivity increases from 4.4 to 5.2. As mentioned, a possible explanation for the increases in permeability associated with no changes or increases in selectivity could be in the amount of cross-linked polymer, since PNPr membrane cross-linked for 1 h is made up of 96.4% GC, whereas the one cross-linked for 24 h contains 98.5% GC of cross-linked polymer.

Table 2 shows the d -spacing values for these two membranes, the ones cross-linked at 190 °C for 1 and 24 h. Their values reveal that the net effect of increasing time is to increase the d -spacing of the loosely packed PNPr chains from 7.90 to 8.02 Å, while at the same time the d -spacing of the more efficiently packed chains decreases from 4.02 to 3.98 Å. Even though the d -spacing is not a direct measurement of the real free volume fraction available for permeation, in general an

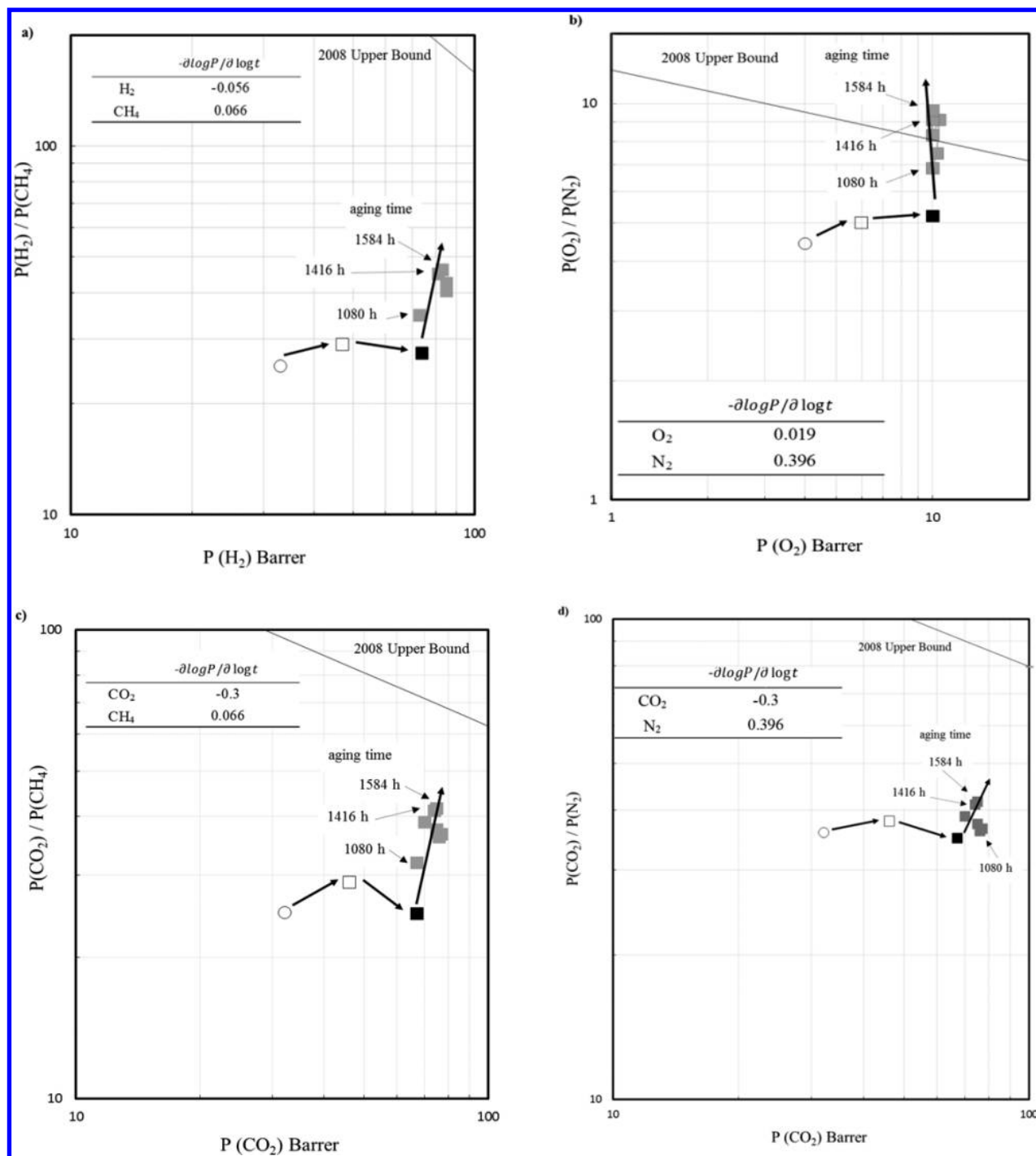


Figure 6. Ideal selectivity–permeability relationship for the gas pairs (a) H₂/CH₄, (b) O₂/N₂, (c) CO₂/CH₄, and (d) CO₂/N₂, at 35 °C and 2 bar, determined for pure PNPr and for PNPr membranes thermally treated at 190 °C for 1 (open squares) and 24 h (black squares). Effect of annealing, at 35 °C under 10⁻³ mmHg vacuum, is also shown for a PNPr cross-linked membrane at 190 °C/24 h (gray squares). Robeson's 2008 upper-bound limit is shown as a reference line.

increase in the largest *d*-spacing, and probably its distribution, seems to favor the permeability of small kinetic diameter gases such as H₂, O₂, and CO₂, whereas the decrease in the smaller *d*-spacing, and probably its distribution, causes smaller increases in the permeability of larger kinetic diameter gases such as N₂ and CH₄ tested here.

Figure 6 shows the effect of aging time, at 35 °C and under vacuum at 10⁻³ mmHg for at least 1584 h, on the selectivity–permeability relationship for a cross-linked PNPr (at 190 °C

for 24 h). The effect of aging time under vacuum shows that the permeability coefficients of the fastest gas slightly increase, i.e., *P*(H₂) and *P*(CO₂), or remain constant, i.e., *P*(O₂), during the 1584 h, but interestingly the selectivities for the gas pairs with respect to CH₄ and N₂ show important increases depending on the type of gases. For the gas pairs H₂/CH₄ and CO₂/CH₄, *P*(H₂) and *P*(CO₂) increase by 1.11 and 1.04 factors, respectively, and their associated selectivities increase from 24 to 45 for H₂/CH₄ and from 22 to 39 for CO₂/CH₄.

For O_2/N_2 , $P(O_2)$ remains practically constant after aging for 1584 h, and its selectivity increases from 5.2 to 9.6, a selectivity–permeability combination that surpasses the 2008 upper-bound limit.⁶ This is an interesting result because it indicates that the effect of cross-linking, added to a vacuum-annealing period, leads to membranes that overcome the typical trade-off observed between selectivity and permeability. In effect, these cross-linked membranes annealed at 35 °C and under vacuum for 1584 h show $P(H_2)$ and $P(CO_2)$ increases that are 2.45 and 2.11 times the one found for the non-cross-linked membranes, and they have associated increases in selectivity that almost double from 25 to 45 for H_2/CH_4 and from 25 to 39 for CO_2/CH_4 . For the gas pair O_2/N_2 , $P(O_2)$ increases by a 2.4 factor and its selectivity increases from 4.4 to 9.6 after cross-linking and annealing under vacuum.

Finally, Figure 7 shows the effect of CO_2 upstream pressure on $P(CO_2)$ measured for PNPr cross-linked membranes at 190

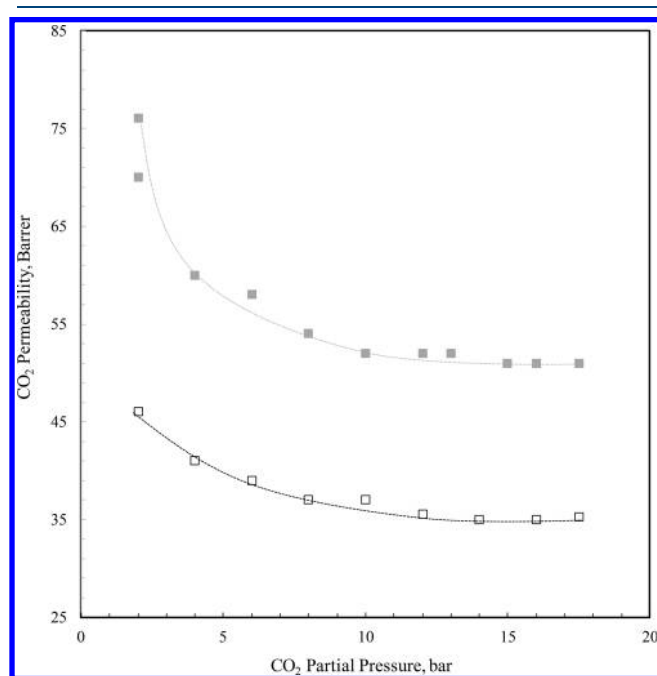


Figure 7. Effect of CO_2 upstream pressure on CO_2 permeability coefficient for PNPr membranes cross-linked at 190 °C for 1 h (open squares) and for 24 h plus an additional annealing period, at 35 °C under 10^{-3} mmHg vacuum, of 1584 h (gray squares).

°C for 1 h without annealing, as well as for those membranes that have been cross-linked for 24 h and vacuum-annealed at 35 °C for the 1584 h period. The results shows that the cross-linked membranes also possess a high resistance to CO_2 plasticization at least up to the 18 bar upstream pressure measured in this work.

4. CONCLUSIONS

A poly(oxyindole biphenylene) containing a cross-linkable propargyl group (PNPr) was successfully synthesized at room temperature. The PNPr was cross-linked, under vacuum (1 mmHg), at temperatures between 190 and 210 °C for periods of time of 1 and 24 h. The cross-linking time increases the GC [%] and the permeability coefficients with practically no changes or increases in selectivity depending on the gas pair to be separated. For cross-linked PNPr membranes at 190 °C, the GC [%] increases from 96.4% in 1 h to 98.5% for 24 h. The gas

permeability coefficients increase, with GC [%], by 2.2 and 2.1 factors for $P(H_2)$ and $P(CO_2)$, whereas selectivity remains constant at 25–27 for H_2/CH_4 and CO_2/CH_4 . Under the same cross-linking treatment $P(O_2)$ increases by a 2.5 factor with an increase in selectivity that goes from 4.4 to 5.2. The cross-linked PNPr membranes are physically resistant to solvent-swelling since their SD [%], in an aggressive solvent such as NMP, is on the order of 1–3%. This represents a tremendous advantage since the non-cross-linked PNPr, which is soluble in common solvents such as CH_2Cl_2 and NMP, can be processed as a cast film and further cross-linked as a quite resistant membrane to solvent-swelling. Throughout a systematic study of the structure/processing/property relationship supported with FTIR-ATR, specific volume, WAXD, and permeability coefficient determinations, it is concluded that cross-linking followed with an additional 1584 h vacuum-annealing period at 35 °C under a 10^{-3} mmHg vacuum is a useful route to produce cross-linked PNPr membranes that can surpass the typical trade-off observed in the permeability–selectivity relationship. When the PNPr membranes, cross-linked at 190 °C for 24 h and further vacuum-annealed at 35 °C for 1584 h, are compared to the non-cross-linked PNPr membranes, both $P(H_2)$ and $P(CO_2)$ increase by 2.4 and 2.2 factors and selectivity for H_2/CH_4 increases from 25 to 45 and for CO_2/CH_4 increases from 25 to 39. It was also found that $P(O_2)$ increases by a 2.3 factor with a corresponding increase for O_2/N_2 selectivity from 4.4 to 9.6, positioning this membrane above the Robeson's 2008 upper-bound limit⁶ at least for this gas pair. Additionally, the cross-linked membranes also possess an acceptable physical resistance to CO_2 plasticization since the plasticization pressure is not detected up to 18 bar upstream pressure.

■ AUTHOR INFORMATION

Corresponding Author

*Tel.: +52(55)5950-4000, ext 4742. E-mail alberto.ruiz@ibero.mx.

ORCID

F. Alberto Ruiz-Treviño: 0000-0002-6476-8137

Manuel J. Aguilar-Vega: 0000-0002-8473-3628

Mikhail G. Zolotukhin: 0000-0001-7395-7354

Notes

The authors declare no competing financial interest.

■ ACKNOWLEDGMENTS

The authors acknowledge financial support from CONACYT Grant CB-2012-01-184156 and 251693 and DGAPA-UNAM (PAPIIT and IN203517). Jesús Ortiz-Espinoza thanks CONACYT and Universidad Iberoamericana for the scholarship. Thanks are due to E. R. Morales, S. Morales, A. Lopez Vivas, and Alejandro Pompa for technical help.

■ REFERENCES

- (1) Hinchliffe, A. B.; Porter, K. E. A comparison of membrane separation and distillation. *Trans. Inst. Chem. Eng.* **2000**, *78*, 255–268.
- (2) Alqaheem, Y.; Alomair, A.; Vinoba, M.; Pérez, A. Polymeric Gas-Separation Membranes for Petroleum Refining. *Int. J. Polym. Sci.* **2017**, *2017*, 4250927.
- (3) Baker, R. W.; Low, B. T. Gas separation membrane materials: a perspective. *Macromolecules* **2014**, *47* (20), 6999–7013.
- (4) Baker, W. R. Future Directions of Membrane Gas Separation Technology. *Ind. Eng. Chem. Res.* **2002**, *41*, 1393–1411.

- (5) Hu, C. C.; Chang, C. S.; Ruaan, R. C.; Lai, J. Y. Effect of free volume and sorption on membrane gas transport. *J. Membr. Sci.* **2003**, *226*, 51–61.
- (6) Robeson, L. M. The upper bound revisited. *J. Membr. Sci.* **2008**, *320*, 390–400.
- (7) Lin, H.; Yavari, M. Upper bound of polymeric membranes for mixed-gas CO₂/CH₄ separations. *J. Membr. Sci.* **2015**, *475*, 101–109.
- (8) Chung, T. S.; Ren, J.; Wang, R.; Li, D.; Liu, Y.; Pramoda, K. P.; Cao, C.; Loh, W. W. Development of asymmetric 6FDA-2,6DAT hollow fiber membranes for CO₂/CH₄ separation: Part 2. Suppression of plasticization. *J. Membr. Sci.* **2003**, *214*, 57–69.
- (9) Dong, G.; Li, H.; Chen, V. Plasticization mechanisms and effects of thermal annealing of Matrimid hollow fiber membranes for CO₂ removal. *J. Membr. Sci.* **2011**, *369*, 206–220.
- (10) Sanders, D. F.; Smith, Z. P.; Ribeiro, C. P., Jr.; Guo, R.; McGrath, J. E.; Paul, D. R.; Freeman, B. D. Gas permeability, diffusivity, and free volume of thermally rearranged polymers based on 3,3'-dihydroxy-4,4'-diamino-biphenyl (HAB) and 2,2'-bis-(3,4-dicarboxyphenyl) hexafluoropropane dianhydride (6FDA). *J. Membr. Sci.* **2012**, *409-410*, 232–241.
- (11) Wiegand, J. R.; Smith, Z. P.; Liu, Q.; Patterson, C. T.; Freeman, B. D.; Guo, R. Synthesis and characterization of triptycene-based polyimides with tunable high fractional free volume for gas separation membranes. *J. Mater. Chem. A* **2014**, *2*, 13309–13320.
- (12) Bengtson, G.; Neumann, S.; Filiz, V. Membranes of Polymers of Intrinsic Microporosity (PIM-1) Modified by Poly (ethylene glycol). *Membranes* **2017**, *7* (2), 28.
- (13) Bos, A.; Punt, I. G. M.; Wessling, M.; Strathmann, H. CO₂ induced plasticization phenomena in glassy polymers. *J. Membr. Sci.* **1999**, *155*, 67–78.
- (14) Chiou, S. J.; Barlow, W. J.; Paul, D. R. Plasticization of glassy polymers by CO₂. *J. Appl. Polym. Sci.* **1985**, *30*, 2633–2642.
- (15) Sanders, E. S. Penetrant-induced plasticization and gas permeation in glassy polymers. *J. Membr. Sci.* **1988**, *37*, 63–80.
- (16) Wessling, M.; Huisman, I.; Boomgaard, Th. v. d.; Smolders, C. A. Smolders C.A Dilation kinetics of glassy, aromatic polyimides induced by carbon dioxide sorption. *J. Polym. Sci., Part B: Polym. Phys.* **1995**, *33*, 1371–1384.
- (17) Staudt-Bickel, C.; Koros, W. J. Improvement of CO₂/CH₄ separation characteristics of polyimides by chemical crosslinking. *J. Membr. Sci.* **1999**, *155*, 145–154.
- (18) Staiger, C. L.; Pas, S. J.; Hill, A. J.; Cornelius, C. J. Gas Separation, Free Volume Distribution, and Physical Aging of a Highly Microporous Spirobisindane Polymer. *Chem. Mater.* **2008**, *20*, 2606–2608.
- (19) Cao, C.; Chung, T. S.; Liu, Y.; Wang, R.; Pramoda, K. P. Chemical cross-linking modification of 6FDA-2,6-DAT hollow fiber membranes for natural gas separation. *J. Membr. Sci.* **2003**, *216*, 257–268.
- (20) Wind, J. D.; Paul, D. R.; Koros, W. J. Natural gas permeation in polyimide membranes. *J. Membr. Sci.* **2004**, *228*, 227–236.
- (21) Ward, J. K.; Koros, W. J. Crosslinkable mixed matrix membranes with surface modified molecular sieves for natural gas purification: I. Preparation and experimental results. *J. Membr. Sci.* **2011**, *377*, 75–81.
- (22) Wind, J. D.; Staudt-Bickel, C.; Paul, D. R.; Koros, W. J. The Effects of Crosslinking Chemistry on CO₂ Plasticization of Polyimide Gas Separation Membranes. *Ind. Eng. Chem. Res.* **2002**, *41*, 6139–6148.
- (23) Song, Q.; Cao, S.; Pritchard, H. R.; Ghalei, B.; Al-Muhtaseb, S. A.; Terentjev, M. E.; Cheetham, K. A.; Sivaniah, E. Controlled thermal oxidative crosslinking of polymers of intrinsic microporosity towards tunable molecular sieve membranes. *Nat. Commun.* **2014**, *5*, 4813.
- (24) Ghanem, B. S.; Swaidan, R.; Litwiller, E.; Pinnau, I. Ultramicroporous triptycene-based polyimide membranes for high-performance gas separation. *Adv. Mater.* **2014**, *26*, 3688–3692.
- (25) Hernández-Martínez, H.; Ruiz-Treviño, F. A.; Ortiz-Espinoza, J.; Aguilar-Vega, M. J.; Zolotukhin, M. G.; Marcial-Hernandez, R.; Olvera, L. I. Simultaneous Thermal Cross-Linking and Decomposition of Side Groups to Mitigate Physical Aging in Poly(oxyindole biphenylene) Gas Separation Membranes. *Ind. Eng. Chem. Res.* **2018**, *57*, 4640–4650.
- (26) Çaykara, T.; Akçakaya, I. Synthesis and network structure of ionic poly(N,N dimethylacrylamide-co-acrylamide) hydrogels: Comparison of swelling degree with theory. *Eur. Polym. J.* **2006**, *42*, 1437–1445.
- (27) Camacho-Zuñiga, C.; Ruiz-Treviño, F. A.; Zolotukhin, M. G.; Del Castillo, L. F.; Guzmán, J.; et al. Gas transport properties of new aromatic cardo poly(aryl ether ketone)s. *J. Membr. Sci.* **2006**, *283*, 393–398.
- (28) Hernandez, M. C. G.; Zolotukhin, M. G.; Fomine, S.; Cedillo, G.; Morales, S. L.; Frohlich, N.; Preis, E.; Scherf, U.; Salmon, M.; Chavez, M. I.; Cardenas, J.; Ruiz-Trevino, A. Novel, metal-free, superacid-catalyzed “click” reactions of isatins with linear, non-activated, multiring aromatic hydrocarbons. *Macromolecules* **2010**, *43*, 6968–6979.
- (29) Dogan-Demir, K.; Kiskan, B.; Yagci, Y. Thermally curable acetylene-containing main-chain benzoxazine polymers via sonogashira coupling reaction. *Macromolecules* **2011**, *44* (7), 1801–1807.
- (30) Greenwood, T. D.; Armistead, D. M.; Wolfe, J. F.; St Clair, A. K.; St Clair, T. L.; Barrick, J. D. N-Propargyl-substituted aromatic polyamides: preparation and thermal crosslinking. *Polymer* **1982**, *23*, 621–625.
- (31) Gao, Y.; Huang, F.; Zhou, Y.; Du, L. Synthesis and Characterization of a Novel Acetylene- and Maleimide- Terminated Benzoxazine and Its High-Performance Thermosets. *J. Appl. Polym. Sci.* **2013**, *128*, 340–346.
- (32) Secker, C.; Brosnan, S. M.; Limberg, F. R.; Braun, U.; Trunk, M.; Strauch, P.; Schlaad, H. Thermally induced crosslinking of poly (N-propargyl glycine). *Macromol. Chem. Phys.* **2015**, *216* (21), 2080–2085.
- (33) Pixton, R. M.; Paul, D. R. Gas Transport Properties of Polyarylates Part II: Tetrabromination of the Bisphenol. *J. Polym. Sci., Part B: Polym. Phys.* **1995**, *33*, 1353–1364.
- (34) Jeon, J. W.; Kim, D.-G.; Sohn, E.; Yoo, Y.; Kim, Y. S.; Kim, B. G.; Lee, J.-C. Highly Carboxylate-Functionalized Polymers of Intrinsic Microporosity for CO₂-Selective Polymer Membranes. *Macromolecules* **2017**, *50*, 8019–8027.
- (35) Weber, J.; Su, Q.; Antonietti, M.; Thomas, A. Exploring Polymers of Intrinsic Microporosity—Microporous, Soluble Polyamide and Polyimide. *Macromol. Rapid Commun.* **2007**, *28*, 1871–1876.